



Title	New plasma surface-treated memory alloys: Towards a new generation of "smart" orthopaedic materials
Author(s)	Yeung, KWK; Chan, YL; Lam, KO; Liu, XM; Wu, SL; Liu, XY; Chung, CY; Lu, WW; Chan, D; Luk, KDK; Chu, PK; Cheung, KMC
Citation	Advanced Processing of Biomaterials Symposium, Materials Science and Technology Conference and Exhibition, Cincinnati, Ohio, USA, 15–19 October 2006. In Materials Science And Engineering C, 2008, v. 28 n. 3, p. 454-459
Issued Date	2008
URL	http://hdl.handle.net/10722/68265
Rights	NOTICE: this is the author's version of a work that was accepted for publication in Materials Science and Engineering C: Biomimetic Materials, Sensors and Systems. Changes resulting from the publishing process, such as peer review, editing, corrections, structural formatting, and other quality control mechanisms may not be reflected in this document. Changes may have been made to this work since it was submitted for publication. A definitive version was subsequently published in Materials Science and Engineering C: Biomimetic Materials, Sensors and Systems, 2008, v. 28 n. 3, p. 454-459. DOI: 10.1016/j.msec.2007.04.023



ELSEVIER

Available online at www.sciencedirect.com



Materials Science and Engineering C xx (2007) xxx–xxx



www.elsevier.com/locate/msec

1

2

3

New plasma surface-treated memory alloys: Towards a new generation of “smart” orthopaedic materials

4

K.W.K. Yeung^a, Y.L. Chan^a, K.O. Lam, X.M. Liu^b, S.L. Wu^b, X.Y. Liu^b, C.Y. Chung^b,
W.W. Lu^a, D. Chan^c, K.D.K. Luk^a, Paul K. Chu^{b,*}, K.M.C. Cheung^{a,*}

5

6

^a Department of Orthopaedics and Traumatology, The University of Hong Kong, Pokfulam, Hong Kong, China

7

^b Department of Physics and Materials Science, City University of Hong Kong, Tat Chee Avenue, Kowloon Tong, Hong Kong, China

8

^c Department of Biochemistry, The University of Hong Kong, Pokfulam, Hong Kong, China

9

Abstract

10

This paper describes the corrosion resistance, surface mechanical properties, cyto-compatibility, and *in-vivo* performance of plasma-treated and untreated NiTi samples. Nickel–titanium discs containing 50.8% Ni were treated by nitrogen and carbon plasma immersion ion implantation (PIII). After nitrogen plasma treatment, a layer of stable titanium nitride is formed on the NiTi surface. Titanium carbide is also found at the surface after carbon plasma implantation. Compared to the untreated samples, the corrosion resistances of the plasma PIII samples are better by a factor of five and the surface hardness and elastic modulus are better by a factor of two. The concentration of Ni leached into the simulated body fluids from the untreated samples is 30 ppm, whereas that from the plasma-treated PIII are undetectable. Although there is no significant difference in the ability of cells to grow on either surface, bone formation is found to be better on the nitrogen and carbon PIII sample surfaces at post-operation 2 weeks. All these improvements can be attributed to the formation of titanium nitride and titanium carbide on the surface.

11

12

13

14

15

16

17

18

© 2007 Published by Elsevier B.V.

19

20

Keywords: Plasma immersion ion implantation; Corrosion resistance; NiTi

21

1. Introduction

22

Nickel–titanium (NiTi) shape memory alloy is an attractive orthopaedic metallic material due to its two intrinsic properties (shape memory effect (SME) and super-elasticity (SE)) that may not be found in other commonly-used surgical metals. The biocompatibility of this material has been proved by many studies [1–12]. However, some adverse effects such as inferior osteogenesis process, lower osteonectin synthesis activity and higher cell death rate have also been reported [13–16]. All these problems are attributed to an increase in cytotoxicity due

23

24

25

26

27

28

29

30

31

to poor corrosion resistance. Additionally, one important issue is that the nickel ions released from the alloys can cause detrimental effect to humans, particularly in nickel hypersensitive patients resulting in strong allergic reactions [5,6,17–20]. Not surprisingly, the anti-corrosion property and wear resistance of NiTi alloy must be assured before it can be applied for surgical implantation, since fretting at the interface of couplings of orthopaedic implants is always expected. To enhance the corrosion resistance and wear property, the material microstructures and surface morphology must be taken into account. Plasma-based implantation with the use of tantalum and oxygen has been used by previous studies in order to improve the surface mechanical properties of NiTi alloy [21–23]. Our group proposes to enhance the corrosion and wear resistance of NiTi by using nitrogen and carbon plasma immersion ion implantation (PIII). This study aims to compare: (1) the surface mechanical properties; (2) the surface chemistry; (3) osteoblast viability and (4) new bone formation under *in-vivo* conditions of nitrogen PIII NiTi, carbon PIII NiTi and untreated NiTi.

32

33

34

35

36

37

38

39

40

41

42

43

44

45

46

47

48

49

50

51

* Corresponding authors. Cheung is to be contacted at the Department of Orthopaedics and Traumatology, The University of Hong Kong, Pokfulam, Hong Kong, China. Tel.: +852 29740282; fax: +852 28174392. Chu, Department of Physics and Materials Science, City University of Hong Kong, Tat Chee Avenue, Kowloon Tong, Hong Kong, China. Tel.: +852 27887724; fax: +852 27889549.

E-mail addresses: paul.chu@cityu.edu.hk (P.K. Chu), ken-cheung@hku.hk (K.M.C. Cheung).

2. Methodology

Circular NiTi bars with 50.8% Ni (SE508, Nitinol Device Company, Fremont, USA) were prepared into discs (diameter = 5 mm and thickness = 1 mm). All of them were ground and polished to a shiny surface, and then ultrasonically cleaned with acetone and ethanol before plasma implantation [24–26]. The implantation parameters are displayed in Table 1. All the plasma-treated samples were ultrasonically cleaned with acetone and ethanol before surface composition analysis and cell culturing.

Survey scanning mode of X-ray photoelectron spectroscopy (XPS) (Physical electronics PHI 5802 system, Minnesota, USA) was used to examine the surface chemical compositions. The survey scans were acquired after Ar ion sputtering to remove interferences from surface contamination. A monochromatic aluminium X-ray source was employed and the sampled area was 0.8 mm in diameter. The step size for bulk scanning survey was 0.8 eV while the high-resolution narrow scans to confirm the formed elements were obtained with a step of 0.1 eV. The energy scale was calibrated using the Cu2p₃ (932.67 eV) and Cu3p (75.14 eV) peaks from a pure copper standard.

The electrochemical tests [27] based on ASTM G5-94 (1999) and G61-86 (1998) protocols were performed by a potentiostat (VersaStat II EG & G, USA) using a standard simulated body fluid (SBF) at a pH of 7.42 [28] and temperature of 37 ± 0.5 °C. The ion concentrations in the SBF are shown in Table 2 [28]. A cyclic potential spanning between −500 mV and +1500 mV was applied at a scanning rate of 600 mV/h. In accordance with the testing protocol, the medium was purged with nitrogen for 1 h to remove dissolved oxygen before the electrochemical tests. The cyclic potential was scanned after 10 s of delay time during which no potential was applied. The surface morphology of each sample after the test was studied using scanning electron microscopy (SEM) (JEOL JSM-820, Japan). In addition, the solvents were analyzed by inductively-coupled plasma mass spectrometry (ICPMS) (Perkin Elmer, PE SCIEX ELAN6100, USA) after corrosion testing so as to determine the amount of Ni ions leached from each specimen [29].

To investigate the average surface hardness and Young's modulus, nano-indentation tests [29] (MTS Nano Indenter XP,

Table 2

Ion concentration of saturated body fluid in comparison with human blood plasma

	Concentration (Mm)							
	Na ⁺	K ⁺	Ca ²⁺	Mg ²⁺	HCO ₃ ⁻	Cl ⁻	HPO ₄ ²⁻	SO ₄ ²⁻
SBF	142.0	5.0	2.5	1.5	4.2	148.5	1.0	0.5
Blood plasma	142.0	5.0	2.5	1.5	27.0	103.0	1.0	0.5

USA) were conducted on five areas of the samples. A three-sided pyramidal Berkovich diamond indenter was employed. Readings were recorded through a depth of 200 nm during unloading cycle.

To investigate the cyto-compatibility of the plasma-treated and untreated samples, osteoblasts isolated from calvarial bones of 2-day-old mice that ubiquitously expressed an enhanced green fluorescent protein (EGFP) were used in our culture in a Dulbecco's Modified Eagle Medium (DMEM) (Invitrogen) supplemented with 10% (v/v) fetal bovine serum (Biowest, France), antibiotics (100 U/ml of penicillin and 100 µg/ml of streptomycin), and 2 mM L-glutamine at 37 °C in an atmosphere of 5% CO₂ and 95% air. The specimens (1 mm thick and 5 mm in diameter) were fixed onto the bottom of a 24-well tissue culture plate (Falcon) using 1% (w/v) agarose. A cell suspension consisting of 5000 cells was seeded onto the surface of the untreated NiTi, the nitrogen-treated NiTi, and carbon-treated NiTi and wells without any metal discs serving as a control for normal culturing conditions. Cell attachment was examined after the second day of culture. Four samples were used to obtain better statistics. Cell viability was observed by using a fluorescent microscope (Axioplan 2, Carl Zeiss, Germany). The attached living EGFP-expressing osteoblasts were visualized using a 450–490 nm incident filter and the fluorescence images emitted at 510 nm captured using a Sony DKS-ST5 digital camera.

For the animal study, with the approval obtained from our University Ethics Committee, young New Zealand white rabbit of 26 weeks old was used for the surgery. Ketamin (35 mg/kg), xylazine (5 mg/kg) and acepromazine (1 mg/kg) were administrated through intra-muscular injection to anaesthetize the animal. Two holes in 5 mm diameter and 1 mm depth were prepared at the left side of ilium and the great trochanter of femur through minimal incision, whereas the right side with intact bone served as control. The samples were press-fitted into the prepared holes. One rabbit was implanted with two identical samples. Time points were set at 2 and 4 weeks. In each time point, six rabbits were used and divided for untreated NiTi, nitrogen-treated NiTi and carbon-treated NiTi group. Standard post-operative care was carried out to each rabbit according to the testing protocol. Ketofen 3 mg/kg through intra-muscular injection for analgesics for 5 days was done. Terramycin once for 4 days for 2 courses was administrated as antibiotic. By each time point of the *in-vivo* study, animals were sacrificed. Histological examinations of the implanted tissue blocks were performed. For light microscopic examination, alcohol-fixed tissue block samples were embedded in methyl methacrylate (Technovit® 9100 New, Heraeus Kulzer GmbH, Germany).

Table 1

Nitrogen and carbon plasma immersion ion implantation parameters

Sample	NiTi without implantation	NiTi with nitrogen implantation	NiTi with carbon implantation
Gas type	Control	N ₂	C ₂ H ₂
RF	–	1000 W	–
High voltage	–	–40 kV	–40 kV
Pulse width	–	30 µs	30 µs
Frequency	–	50 Hz	200 Hz
Duration of implantation (min)	–	240	90
Base pressure	–	7.0 × 10 ⁻⁶ Torr	1.0 × 10 ⁻⁵ Torr
Working pressure	–	6.4 × 10 ⁻⁴ Torr	2.0 × 10 ⁻³ Torr
Dose	–	1.4 × 10 ¹⁶ cm ⁻²	5.5 × 10 ¹⁶ cm ⁻²

t3.1 Table 3

A summary of elements/compounds present at the topmost surface of the untreated NiTi, nitrogen-treated NiTi, carbon-treated NiTi examined by XPS surface surveying scan

Sample	Element/compound formed on surface (binding energy)
Untreated NiTi	TiO(455 eV), TiO ₂ (458.8 eV), NiO(853.8 eV)
Nitrogen-treated NiTi	TiN(456 eV), TiO ₂ (458.8 eV), NiO(853.8 eV, low amount)
Carbon-treated NiTi	TiC(284.8 eV), TiO ₂ (458.8 eV), NiO(853.8 eV, low amount)

142 Three-micrometer-thick sections were cut and stained with
143 Giemsa and eosin according to standard procedures.

144 3. Results and discussion

145 Surface compounds of the untreated NiTi, nitrogen-treated
146 NiTi and carbon-treated NiTi derived from their binding
147 energies are summarized in Table 3 in accordance with the
148 handbook of XPS analysis [42]. The major compounds found at
149 the untreated NiTi sample surfaces are TiO, TiO₂, and NiO
150 respectively. For the nitrogen-implanted surfaces, TiN and TiO₂
151 are detected. TiC and TiO₂ are found at the surface after carbon
152 plasma implantation. The depth profiles (data not shown here)
153 of the nitrogen- and carbon-treated samples suggest that the NiO
154 concentration is little as compared with that on the untreated
155 one. The findings therefore suggest that the superficial Ni
156 concentration is depleted after plasma treatment.

157 Fig. 1 shows the results of surface Young's modulus of the
158 untreated and implanted samples. The moduli of nitrogen- and
159 carbon-treated sample are about 105 GPa and 110 GPa res-
160 pectively, whereas the untreated sample only survived at
161 55 GPa. Fig. 2 reveals the hardness testing results. The surface
162 harnesses after nitrogen and carbon plasma implantation are
163 8 GPa and 7 GPa, separately. The hardness of the untreated
164 sample only is found at 4.5 GPa. In general, the modulus and
165 hardness have doubled after plasma treatment. Although the
166 thickness of those implanted layers are only 60 nm for nitrogen-
167 implanted sample and 120 nm described by XPS depth-
168 profiling (data not shown), it seems that the increase is mainly
169 contributed by the formation of TiC and TiN as compared with
170 the untreated NiTi.

171 The essential readings from our electrochemical tests in lieu
172 of the complete potentiodynamic curves are shown on Fig. 3.

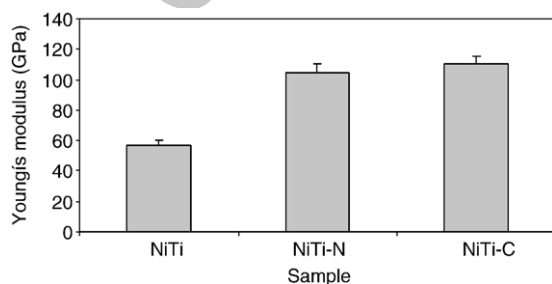


Fig. 1. Surface Young's modulus of the untreated NiTi, nitrogen-treated NiTi and carbon-treated NiTi.

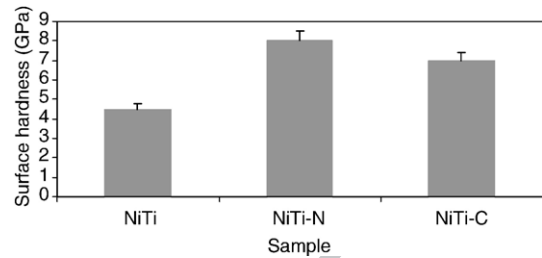


Fig. 2. Surface hardness of the untreated NiTi, nitrogen-treated NiTi and carbon-treated NiTi.

The breakdown potentials measured from the untreated, nitrogen- and carbon-treated NiTi sample are 280 mV, 1080 mV, and 1160 mV, respectively. Larger breakdown potential represent better corrosion resistance. Therefore, the corrosion resistance of the three samples in descending order is carbon-treated NiTi > nitrogen-treated NiTi >> untreated NiTi. The nitrogen- and carbon-treated samples exhibit higher breakdown potential than the untreated NiTi. Fig. 4 shows the Ni ion concentration leached from the substrate after corrosion testing. The ion concentrations are determined by inductively-coupled plasma mass spectrometry (ICPMS). The amount of Ni ion leached from the untreated sample after corrosion testing is about 30 ppm, whereas no significant amount of Ni ions has been found at the plasma-treated samples. Additionally, the surface morphologies of the samples after electrochemical tests are shown in Fig. 5. The holes on the plasma-treated surfaces are very small, whereas much bigger holes with irregular shapes are found on the surface of untreated NiTi. These results suggest that the corrosion resistances of the plasma-treated samples are significantly improved after plasma treatment.

The cell attachments observed on the untreated NiTi, nitrogen-treated NiTi and carbon-treated NiTi samples after 2 days of culturing are shown in Fig. 6. This observation suggests that cells are attached to and started to proliferate on all the samples. The results of cell culturing unequivocally demonstrate that there is no immediate short term cyto-toxic effects on the plasma-treated NiTi samples. The mouse osteoblasts can survive on the plasma-treated and untreated surface.

The *in-vivo* bone formation observed on untreated NiTi, nitrogen-treated and carbon-treated NiTi samples after 2 and 4 weeks of operation are shown in Figs. 7 and 8, respectively. In Fig. 7A, a layer of fibrous tissue is found at the surface of

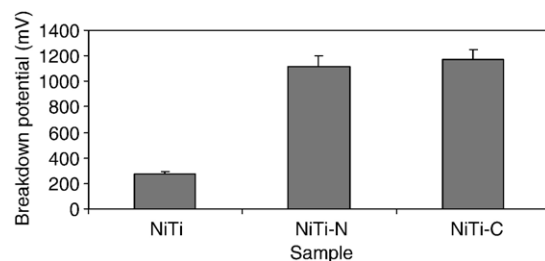


Fig. 3. Breakdown potentials of the untreated NiTi, nitrogen-treated NiTi and carbon-treated NiTi.

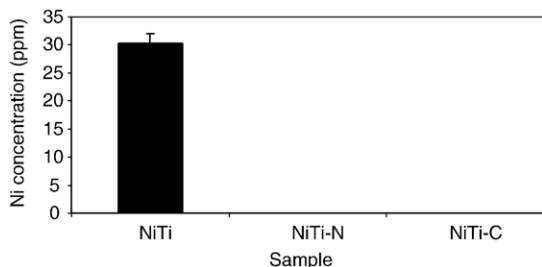


Fig. 4. Ni concentration in the solvent after corrosion testing. The amounts of leached Ni ions from the metals were measured by ICPMS. There was no significant Ni ion found at plasma-treated samples.

untreated NiTi after 2 weeks of implantation. However, a layer
of new bone can be found at the nitrogen- and carbon-treated
NiTi samples shown at Fig. 7B and C, respectively. At 4 weeks
of post-implantation more new bone formations are found at the
nitrogen- and carbon-treated NiTi samples (Fig. 8B and C). For

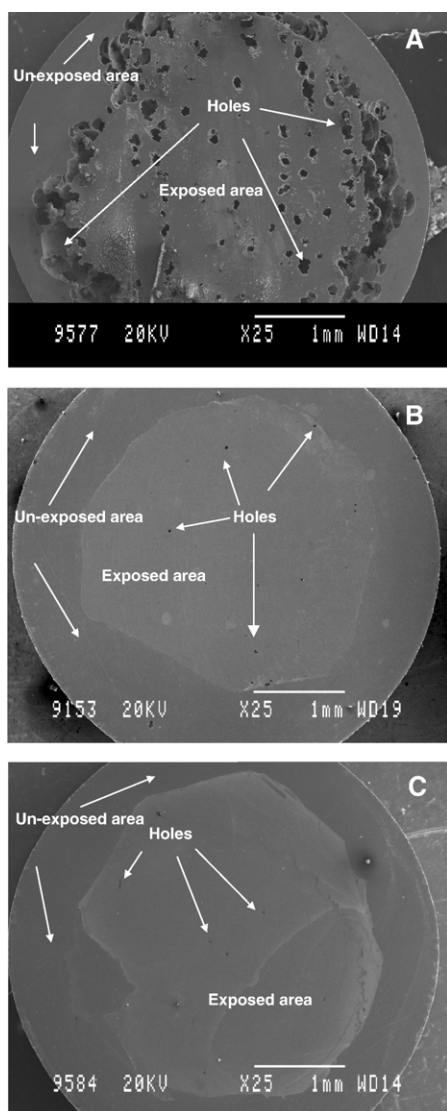


Fig. 5. Microscopic view of the (A) untreated NiTi, (B) nitrogen-treated NiTi and (C) carbon-treated NiTi after electrochemical testing under scanning electron microscopy (SEM) examination.

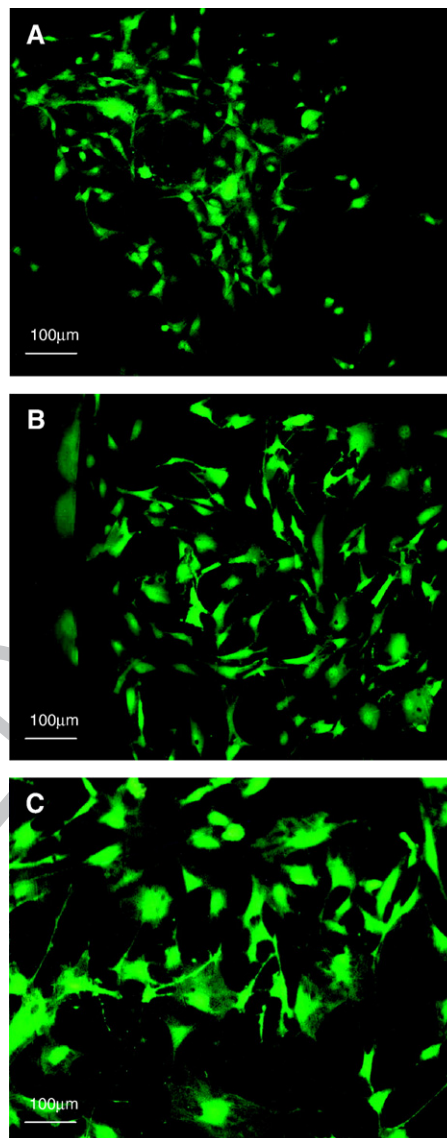


Fig. 6. Microscopic view of the (A) untreated NiTi, (B) nitrogen-treated NiTi and (C) carbon-treated NiTi after 2 days of cell culture using the EGFP-expressing mouse osteoblasts.

the untreated control, bone formation is observed as well at
week 4 of post-operation (Fig. 8A). These results suggest that
the plasma-treated samples are favorable for early bone
formation under *in-vivo* environment rather than the untreated
sample does. However, it does not imply that the untreated
control is incompatible with living tissues. The issue addressed
here is that delayed bone formation is found at the untreated
sample.

Nitrogen and carbon plasma treatments produce a thin layer
of TiN and TiC on the surface together with a graded interface
with the bulk NiTi substrate. Other previous studies [30–34]
applying the plasma surface treatment to enhance the surface
mechanical properties of Ti alloys and stainless steels have been
seen. Few studies [35,36] applying oxygen plasma treatment to
enhance the corrosion and wear resistance of NiTi alloy have
also been found. Their results comply with our surface
mechanical testing data. However, it seems that very little

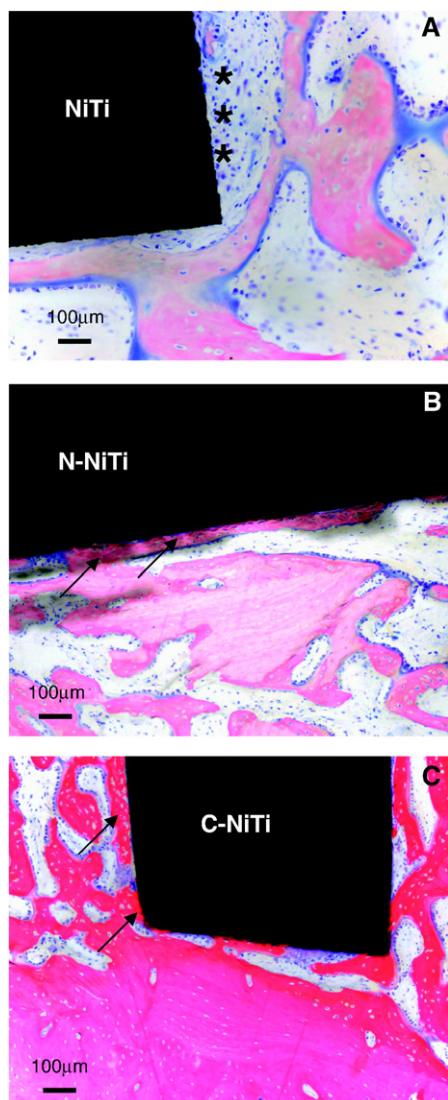


Fig. 7. Giemsa–eosin stained cross-sections of (A) untreated NiTi, (B) nitrogen-treated NiTi and (C) carbon-treated NiTi at post-operation 2 weeks implanted onto the ilium. New bone formation (arrow heads) is found at (B) nitrogen-treated and (C) carbon-treated NiTi. The untreated NiTi (A, asterisk) is only found fibrous tissues formation.

228 previous studies have investigated the properties of the plasma-
 229 treated surfaces starting from *in-vitro* to *in-vivo* systemically.
 230 Therefore, this study somewhat provides a comprehensive in-
 231 formation of nitrogen and carbon plasma-treated surfaces from
 232 surface mechanical properties to *in-vitro* and *in-vivo* properties.

233 Using NiTi in surgical implantation is controversial due to its
 234 high nickel concentration as compared with the medical grade
 235 titanium alloys. Nickel ion leaching from implants has been
 236 reported in previous clinical trial [37]. Some of *in-vivo* and *in-vitro*
 237 studies indicate that cell proliferation on non-surface-treated NiTi
 238 samples is lower compared to other current use medical grade
 239 metals [38]. However, our cell culturing results show that the
 240 osteoblasts can survive on the plasma-treated and untreated NiTi
 241 samples after 2 days of culturing. In addition to superior surface
 242 mechanical properties [39,40], the plasma-treated NiTi samples
 243 favor new bone formation at the first 2 weeks. In the literature

the TiN and TiC coatings are well tolerated by different cells, 244
 particularly bone cells [30,33,37,41]. This phenomenon can be 245
 attributed to the growth of the calcium phosphate phase on the 246
 surface of titanium nitride coated titanium implant, whereas such 247
 activities do not take place on the untreated titanium implants [31]. 248
 In accordance with the literature [31], this coating is favorable 249
 to bone-like material formation under *in-vivo* conditions. Czar- 250
 nowska et al. [30] confirmed our results that the nitriding layer 251
 possesses better cell proliferation over the untreated layer with 252
 oxide. 253

Generally, plasma immersion ion implantation is a superior 254
 surface modification technology to improve the surface me- 255
 chanical properties and *in-vitro* and *in-vivo* performances of 256
 medical implants, especially implants with complicated geom- 257
 etry [30]. However, this report only reveals the short term cyto- 258

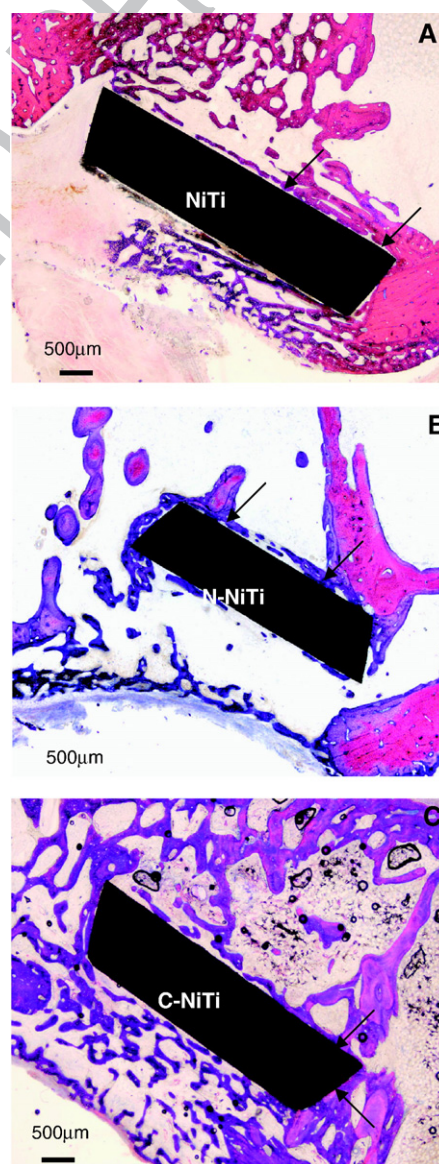


Fig. 8. Giemsa–eosin stained cross-sections of (A) untreated NiTi, (B) nitrogen-treated NiTi and (C) carbon-treated NiTi at post-operation 4 weeks implanted onto the ilium. New bone formation (arrow heads) is found at (A) untreated NiTi, (B) nitrogen-treated and (C) carbon-treated NiTi.

259 compatibility and bone formation effects on those plasma-
260 treated samples. A long term biocompatibility and animal test
261 up to a year is essential prior to applying these surface-treated
262 materials for clinical use.

263 4. Conclusion

264 This study reveals that the layer of TiN and TiC can be formed
265 on the surface of NiTi alloy after nitrogen and carbon plasma
266 treatment. These layers can actually enhance the surface
267 mechanical properties in terms of corrosion and wear as com-
268 pared with the untreated control. *In-vitro* and *in-vivo* studies
269 suggest that nitrogen and carbon plasma-treated surfaces are
270 favorable to osteoblast attachment and bone formation. These
271 surface-treated materials can be actually applied for clinical use if
272 no adverse effect will be found in long term *in-vitro* and *in-vivo*
273 studies.

274 Acknowledgements

275 Financial support from the Hong Kong Research Grant
276 Council (RGC) Central Allocation Grant # CityU 1/04C, Hong
277 Kong Innovation Technology Fund #GHP/019/05, City Univer-
278 sity of Hong Kong Applied Research Grant (ARG) # 9667002,
279 Scoliosis Research Society Standard Investigator Grant, and
280 Hong Kong Innovation Technology Fund #GHP 019/05 is ac-
281 knowledged. The authors also thank Mr. P.W.L Wong for his
282 contribution on the histological work.

283 References

284 [1] D. Bogdanski, M. Koller, D. Muller, G. Muhr, M. Bram, H.P. Buchkremer,
285 D. Stover, J. Choi, M. Epple, *Biomaterials* 23 (2002) 4549.
286 [2] L. El Medawar, P. Rocher, J.-C. Hornez, M. Traisnel, J. Breme, H.F.
287 Hildebrand, *Biomolecular Engineering* 19 (2002) 153.
288 [3] M. Es-Souni, M. Es-Souni, H.F. Brandies, *Biomaterials* 22 (2001) 2153.
289 [4] J. Putters, S. Kaulesar, Z. De, A. Bijma, P. Besseling, *European Surgical*
290 *Research* 24 (1992) 378.
291 [5] A. Kapanen, J. Ilvesaro, A. Danilov, J. Ryhanen, P. Lehenkari, J. Tuukkanen,
292 *Biomaterials* 23 (2002) 645.
293 [6] A. Kapanen, A. Kinnunen, J. Ryhanen, J. Tuukkanen, *Biomaterials* 23
294 (2002) 3341.
295 [7] A. Kapanen, J. Ryhanen, A. Danilov, J. Tuukkanen, *Biomaterials* 22
296 (2001) 2475.
297 [8] S. Kujala, A. Pajala, M. Kallioinen, A. Pramila, J. Tuukkanen, J. Ryhanen,
298 *Biomaterials* 25 (2004) 353.
299 [9] P. Rocher, L. El Medawar, J.-C. Hornez, M. Traisnel, J. Breme, H.F.
300 Hildebrand, *Scripta Materialia* 50 (2004) 255.
301 [10] J. Ryhanen, M. Kallioinen, J. Tuukkanen, J. Junila, E. Niemela, P. Sandvik,
302 W. Serlo, *Journal of Biomedical Materials Research* 41 (1998) 481.
303 [11] J. Ryhanen, E. Niemi, W. Serlo, E. Niemela, P. Sandvik, H. Pernu, T. Salo,
304 *Journal of Biomedical Materials Research* 35 (1997) 451.
305 [12] D.J. Wever, A.G. Veldhuizen, M.M. Sanders, J.M. Schakenraad, J.R. van
306 Horn, *Biomaterials* 18 (1997) 1115.
307 [13] M. Berger-Gorbet, B. Broxup, C. Rivard, L.H. Yahia, *Journal of*
308 *Biomedical Materials Research*. 32 (1996) 243.
371

[14] W. Jia, M.W. Beatty, R.A. Reinhardt, T.M. Petro, D.M. Cohen, C.R. Maze, E.A. Strom, M. Hoffman, *Journal of Biomedical Materials Research*. 48 (1999) 488. 309
310
[15] M. Es-Souni, M. Es-Souni, H. Fischer-Brandies, *Biomaterials* 23 (2002) 2887. 311
312
[16] C.-C. Shih, S.-J. Lin, Y.-L. Chen, Y.-Y. Su, S.-T. Lai, G.J. Wu, C.-F. Kwok, K.-H. Chung, *Journal of Biomedical Materials Research* 52 (2000) 395. 313
314
[17] L. Dalmau, H. Alberty, J. Parra, *Journal of Prosthetic Dentistry* 52 (1984) 116. 315
316
[18] I. Lamster, D. Kalfus, P. Steigerwald, A. Chasens, *Journal of Periodontology* 58 (1987) 486. 317
318
[19] A. Espana, M.L. Alonso, C. Soria, D. Guimaraens, A. Ledo, *Contact Dermatitis* 21 (1989) 204. 319
320
[20] W.E. Sanford, E. Niboer, in: E. Niboer, J.O. Nriagu (Eds.), *Nickel and Human Health Current Perspectives*, John Wiley & Sons, Inc., Canada, 1992, p. 123. 321
322
[21] L. Tan, R.A. Dodd, W.C. Crone, *Catheterization and Cardiovascular Interventions* 24 (2003) 3931. 323
324
[22] L. Tan, W.C. Crone, *Acta Materialia* 50 (2002) 4449. 325
326
[23] Y. Cheng, C. Wei, K.Y. Gan, L.C. Zhao, *Surface and Coatings Technology* 176 (2004) 261. 327
328
[24] P.K. Chu, *Journal of Vacuum Science & Technology B, Microelectronics and Nanometer Structures* 22 (2004) 289. 329
330
[25] P. Chu, B. Tang, Y. Cheng, P. Ko, *Review of Scientific Instruments* 68 (1997) 1866. 331
332
[26] P. Chu, B. Tang, L. Wang, X. Wang, S. Wang, N. Huang, *Review of Scientific Instruments* 72 (2001) 1660. 333
334
[27] D. Starosvetsky, I. Gotman, *Catheterization and Cardiovascular Interventions* 22 (2001) 1853. 335
336
[28] S. Cho, K. Nakanishi, T. Kokubo, N. Soga, *Journal of the American Ceramic Society* 78 (1995) 1769. 337
338
[29] R.W.Y. Poon, J.P.Y. Ho, X. Liu, C.Y. Chung, P.K. Chu, K.W.K. Yeung, W.W. Lu, K.M.C. Cheung, *Thin Solid Films* 488 (2005) 20. 339
340
[30] E. Czarnowska, T. Wierzchon, A. Maranda-Niedbala, *Journal of Materials Processing Technology* 92–93 (1999) 190. 341
342
[31] S. Piscanec, L. Colombi Ciacchi, E. Vesselli, G. Comelli, O. Sbaizero, S. Meriani, A. De Vita, *Acta Materialia* 52 (2004) 1237. 343
344
[32] J. Narayan, W.D. Fan, R.J. Narayan, P. Tiwari, H.H. Stadelmaier, *Materials Science & Engineering. B, Solid-State Materials for Advanced Technology* 25 (1994) 5. 345
346
[33] K.-T. Rie, T. Stucky, R.A. Silva, E. Leitao, K. Bordji, J.-Y. Jouzeau, D. Mainard, *Surface and Coatings Technology* 74–75 (1995) 973. 347
348
[34] A. Vadiraj, M. Kamaraj, *Materials Science & Engineering. A, Structural Materials: Properties, Microstructure and Processing* 416 (2006) 253. 349
350
[35] S. Mandl, D. Krause, G. Thorwarth, R. Sader, F. Zeilhofer, H.H. Horch, B. Rauschenbach, *Surface and Coatings Technology* 142–144 (2001) 1046. 351
352
[36] S. Mandl, R. Sader, G. Thorwarth, D. Krause, H.-F. Zeilhofer, H.H. Horch, B. Rauschenbach, *Biomolecular Engineering* 19 (2002) 129. 353
354
[37] B.D. Boyan, T.W. Hummert, D.D. Dean, Z. Schwartz, *Biomaterials* 17 (1996) 137. 355
356
[38] L. Ponsonnet, V. Comte, A. Othmane, C. Lagneau, M. Charbonnier, M. Lissac, N. Jaffrezic, *Materials Science & Engineering. C, Biomimetic Materials, Sensors and Systems* 21 (2002) 157. 357
358
[39] T. Girardeau, K. Bouslykhane, J. Mimault, J.P. Villain, P. Chartier, *Thin Solid Films* 283 (1996) 67. 359
360
[40] D.M. Grant, S.M. Green, J.V. Wood, *Acta Metallurgica et Materialia* 43 (1995) 1045. 361
362
[41] B.O. Aronsson, J. Lausmaa, B. Kasemo, *Journal of Biomedical Materials Research* 35 (1997) 49. 363
364
[42] J.F. Moulder, W.F. Stickle, P.E. Sobol, K.D. Bomben, J. Chastain, *Handbook of X-ray Photoelectron Spectroscopy: A Reference Book of Standard Spectra for Identification and Interpretation of XPS Data*, Perkin-Elmer, Physical Electronics Division, Minnesota, 1992. 365
366
367
368
369
370